TESTING THE GLACIAL SUBSTRATE MODEL FOR DOUBLE-LAYERED EJECTA CRATERS ON MARS.

D. K. Weiss and J. W. Head, Department of Geological Sciences, Brown University, Providence, RI 02912, U.S.A. (david_weiss@brown.edu)

Introduction: The martian layered ejecta craters possess unique characteristics relative to the ballistically emplaced ejecta of their lunar and mercurian counterparts: their ejecta deposits display distinct boundaries rather than gradational thicknesses and appear to have been fluidized upon emplacement [1]. The unique ejecta morphology associated with layered ejecta craters is typically attributed to subsurface and/or surface volatiles [1-19] and/or atmospheric-vortex interactions [20-24].

Of the wide variety of layered ejecta craters (e.g. single-layered ejecta, multiple-layered ejecta, low-aspect-ratio layered ejecta, pedestal, double-layered ejecta (DLE) craters are a particularly unusual subclass. DLE craters (Fig. 1) range from ~1 to 35 km in diameter (~8 km on average) and exhibit two ejecta facies; the inner facies is characterized by a distinctive radial texture of parallel ridges and grooves, transverse fissures, and an annular depression at the base of the rim [1,15,19]. DLE craters are located in the mid-high latitudes in both hemispheres [15,19]. Ejecta mobility (EM; ratio of ejecta runout distance from the rim crest/crater radius) has been used to characterize the layered ejecta craters [1-5,25], which typically have EM values of ~1-2. DLE craters exhibit anomalously high EM values compared with other martian layered ejecta morphologies, displaying an average EM of ~3 for the outer ejecta facies, and ~1.5 for the inner ejecta facies [5].

DLE craters have been hypothesized to form through 1) interaction with the martian atmosphere [20,21]; 2) the incorporation of volatiles from within the target materials [5-9,14]; 3) some combination of these factors [5,14,17]; 4) a base surge [7,14, 26]; 5) impact melt overtopping the crater rim [9,27], 6) impact into a subsurface ice layer [15]; 7) impact into a volatile-rich substrate followed by a landslide of the near-rim crest ejecta [28]; or 8) impact and penetration through a surface snow and ice layer, followed by an ice-lubricated landslide off of the structurally uplifted rim-crest [19]. They [19] suggest that the landslide of the inner ejecta facies and the long runout distances of the outer facies are explained by ejecta sliding on a lubricating (low friction) icy surface layer. In the latter two landslide scenarios for DLE inner ejecta facies formation, the grooves on the DLE inner facies are analogous to longitudinal grooves formed on the surfaces of terrestrial landslides [30], particularly those that slide on snow and ice [29,30-32].

We use recently improved frictional models [33] to test the landslide hypothesis.

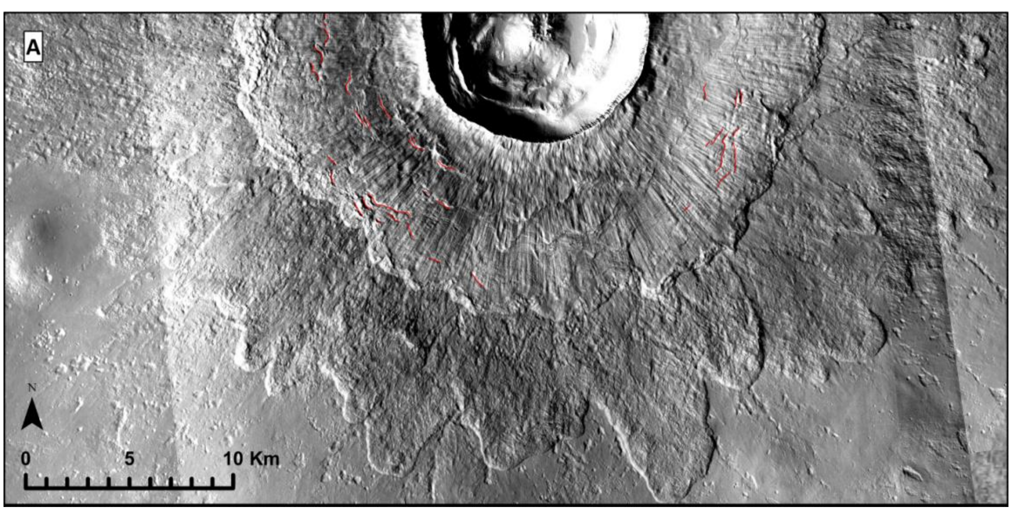

Figure 1. Radial grooves and transverse fissures (red lines) on the southern inner ejecta facies of the martian Steinheim crater (190.6°E, 54.5°N; CTX image P21_009160_2348).

Application of recent quantitative landslide models: DLE inner facies have runout distances of ~2-20 km and initial (rim-crest) heights of ~10-100 m for craters 2 to 25 km in diameter, respectively. Can landslide scaling laws be reconciled with those large runout distances despite their low sliding angles and initial landslide heights? Are the speeds sufficient to form and preserve the grooves, which simultaneously require vertically unmixed flow, low degrees of movement perpendicular to the primary flow direction, low values of basal friction, and high speeds [30,32,34]? Furthermore, did the landslide occur on snow and/or ice (i.e. glacial-substrate model [19]) or rock [28]? In order to address these questions, we model the runout and sliding speeds of a landslide of near rim-crest ejecta. We use the equation of motion for a landslide center of mass (COM) (e.g. [34]) in cylindrical coordinates using the structural uplift height function of [35] and a new frictional weakening law [33].

On the basis of this model, the landslide COM is predicted to have peak sliding speeds ranging between ~12 to 42 m s^{-1}, and average landslide COM speeds ranging between ~8 and 25 m s^{-1} (Fig. 2a). Under the same computational conditions, our results predict landslide durations of 75-675 s (Fig. 2b), depending on crater diameter, over the entire range of input parameters. We find that across the parameter space, the runout distance of the inner ejecta facies COM is predicted to range from 0.4-1.5 R from the rim crest for craters between 2 and 25 km in diameter after correcting for crater collapse (Fig. 2e), and thus are in good agreement with observation. The high EM values of the DLE inner facies, despite low sliding angles and low initial heights, is a predicted consequence of the lubricating snow and ice substrate [4,19]. The average landslide COM speeds calculated (~8-25 m s^{-1}) are typical of, though somewhat lower than, terrestrial landslides overriding glaciers (~20-100 m s^{-1}), which were sufficient to form and preserve grooves. Thus, the presence of grooves on the inner ejecta facies of DLE craters is consistent with a landslide origin. Grooves form through a

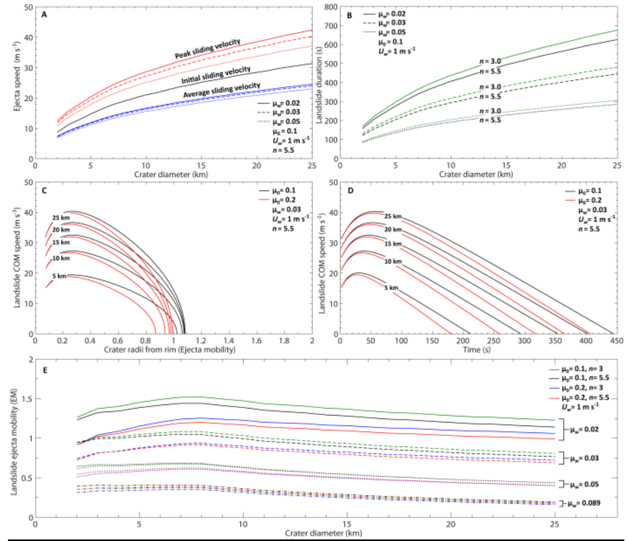

Figure 2. Landslide model results. A) Sliding speed, B) Duration, C, D) Time evolution, E) Runout distance.

shear/splitting process [29,30,32,34] and can only be preserved throughout the landslide under conditions in which the flow is vertically unmixed. Longitudinal grooves (as opposed to more hummocky textures) form when the primary flow direction speed is much greater than the lateral flow speed [32]. We note that in the case of a near rim-crest landslide, azimuthal confinement from adjacent landsliding ejecta will prevent movement at right angles lateral to the primary flow direction, and will thus assist in groove formation Volume in the landslide is thus conserved by splitting, where expansion is accommodated by the longitudinal grooves. This is consistent with the observation that wider are grooves are present with increasing distance from the rim-crest [36].

References: 1) Carr et al., JGR, 1977; 2) Mouginis-Mark, P., JGR, 1979; 3)Costard, F., Earth Moon and Planets, 1989; 4)Weiss, D. and J. Head, Icarus, 2014;5) Barlow, N., Large Met. Impacts III, 2005; 6)Barlow, N., and C. Perez, JGR, 2003; 7)Mouginis-Mark, P., Icarus, 1981; 8)Barlow, N. and T. Bradley, Icarus, 1990; 9)Osinski, G., MAPS, 2006; 10)Wohletz, K., Icarus, 1983; 11)Mouginis-Mark, P., Icarus, 1987; 12)Stewart et al., LPSC 32; 2090, 2001; 13)Baratoux, D., GRL, 2002; 14)Barnouin-Jha et al., JGR, 2005; 15)Boyce, J. and P. Mouginis-Mark, JGR:P, 2006; 16)Senft, L. and S. Stewart, MAPS, 2008; 17)Komatsu et al., JGR:P, 2007; 18)Oberbeck, V., MAPS, 2009;19)Weiss, D. and J. Head, GRL, 2013; 20)Schultz, P. and D. Gault, JGR: SE, 1979; 21)Schultz, P., JGR, 1992; 22)Barnouin-Jh, O. and P. Schultz, JGR:P, 1998; 23)Barnouin-Jha et al., JGR:P, 1999a; 24)Barnouin-Jha et al., JGR:P, 1999b; 25)Barlow, N. and A. Pollak, LPSC 39; 1322, 2002; 26)Harrison et al., LPSC 44; 1702, 2013; 27)Osinski et al., EPSL, 2011; 28)Wulf, G. and T. Kenkmann, LPSC 45; 1792, 2014; 29)Shreve, R., Science, 1966; 30)Dufresne, A. and T. Davies, Geomorph., 2009; 31)Shugar, D. and J. Clague, Sediment., 2011; 32)De Blasio, F., Geomorph., 2014; 33)Lucas et al., Nature Comm., 2014; 34)De Blasio, F., PSS, 2011; 35)Stewart, S. and G. Valiant , MAPS, 2006; 36)Boyce et al., LPSC 45; 1589, 2014.